OUKA

The University of Osaka
Institutional Knowledge Archive

Title	Molecular dynamics simulation of amine groups formation during plasma processing of polystyrene surfaces
Author(s)	Michlíček, Miroslav; Hamaguchi, Satoshi; Zajíčková, Lenka
Citation	Plasma Sources Science and Technology. 2020, 29(10), p. 105020
Version Type	VoR
URL	https://hdl.handle.net/11094/78267
rights	© 2020 The Author(s). Original content from this work may be used under the terms of the Creative Commons Attribution 4.0 licence. Any further distribution of this work must maintain attribution to the author(s) and the title of the work, journal citation and DOI.
Note	

PAPER • OPEN ACCESS

Molecular dynamics simulation of amine groups formation during plasma processing of polystyrene surfaces

View the article online for updates and enhancements.

Molecular dynamics simulation of amine groups formation during plasma processing of polystyrene surfaces

Miroslav Michlíček[1] [ID]**, Satoshi Hamaguchi[2]** [ID] **and Lenka Zajíčková[1,3,*]** [ID]

[1] CEITEC–Central European Institute of Technology & Dept. Phys. Electronics, Faculty of Science, Masaryk University, Žerotínovo nám. 9, Brno 60177, Czech Republic

[2] Center for Atomic and Molecular Technologies, Osaka University, 2-1 Yamadaoka, Suita, Osaka 565-0871, Japan

[3] CEITEC–Central European Institute of Technology, Brno University of Technology, Purkyňova 123, Brno 61200, Czech Republic

E-mail: michlicekm@mail.muni.cz and lenkaz@physics.muni.cz

Abstract

Plasma treatment and plasma polymerization processes aiming to form amine groups on polystyrene surfaces were studied in-silico with molecular dynamics simulations. The simulations were compared with two experiments, (i) plasma treatment in N_2/H_2 bipolar pulsed discharge and (ii) plasma polymerization in cyclopropylamine/Ar radio frequency (RF) capacitively coupled discharge. To model favorable conditions for the incorporation of primary amine groups, we assumed the plasma treatment as the flux of NH_2 radicals and energetic NH_3 ions, and the plasma polymerization as the flux of cyclopropylamine molecules and energetic argon ions. It is shown in both the simulation and the experiment that the polystyrene treatment by the bipolar pulsed N_2/H_2 plasmas with an applied voltage of about ± 1 kV formed a nitrogen-rich layer of a thickness of only a few nm. The simulations also showed that, as the NH_3 incident energy increases, the ratio of primary amines to the total number of N atoms on the surface decreases. It is because the energetic ion bombardment brakes up N–H bonds of primary amines, which are mostly brought to the surface by NH_2 radical adsorption. Our previous experimental work on the CPA plasma polymerization showed that increased RF power invested in the plasma leads to the deposition of films with lower nitrogen content. The MD simulations showed an increase of the nitrogen content with the Ar energy and a limited impact of the energetic bombardment on the retention of primary amines. Thus, the results highlighted the importance of the gas-phase processes on the nitrogen incorporation and primary amines retention in the plasma polymers. However, the higher energy flux towards the growing film clearly decreases amount of hydrogen and increases the polymer cross-linking.

Keywords: amine functionalization, plasma treatment, plasma polymerization, molecular dynamics

S Supplementary material for this article is available online

(Some figures may appear in colour only in the online journal)

---

1. Introduction

Plasma modification of materials by amine groups is promising for applications in which cells interact with the surface as well as for immobilization of proteins and covalent bonding of drugs [1]. The simplest technique relies on introducing amine groups on the polymer surface by plasma treatment in nitrogen (N_2), nitrogen and hydrogen (N_2/H_2) or ammonia (NH_3) discharges [2, 3]. An alternative way to create amine surfaces is plasma deposition, either the co-polymerization of hydrocarbon monomers C_xH_y (e.g., acetylene C_2H_2, ethylene C_2H_4) with NH_3 [4–6] or the plasma polymerization of various monomers containing amine groups [7–13].

Different approaches have been developed to maximize the concentration of the introduced primary amine groups. Plasma treatment of polymers was intensively studied in many configurations, generally showing optimum for a certain power, mixture, pulsing settings and treatment time [14–16]. Plasma-chemical mechanism of primary amine incorporation into hydrocarbons was studied particularly for N_2, N_2/H_2 and NH_3, showing the importance of NH and NH_2 radicals [2, 17]. In absence of hydrogen, the combined action of excited nitrogen $N_2(A)$ and ground state N radical was suggested as a plausible mechanism for the formation of labile nitrogen groups, which subsequently hydrolyze to a primary amine in the open air [17].

A very high specificity of primary amine incorporation was, however, reported only in processes without ion bombardment, such as NH_3 afterglow process ($[NH_2]/[N] > 70\%$, at $[N] \approx 5$ at.%) [3]. Moreover, simple plasma treatment of polymers has only limited stability in time [18]. A possible way to prevent this effect of hydrophobic recovery is to deposit an amine-containing layer.

In the case of plasma polymerization, the high retention of the original precursor is usually achieved by using low specific power which, however, has to be balanced with the film stability [1, 19, 20]. Other approaches have been also reported, recently e.g., method based on the deposition of protonated precursor ions via $\alpha-\gamma$ transition [21]. Despite these efforts, the amine concentration is usually limited to few atomic percent, especially in conditions with treated surface or growing layer subjected to ion bombardment [8, 20, 22–24]. It should be empathized, that reported primary amine concentrations based on TFBA derivatization should be considered as an upper estimate due to possible ambiguity of TFBA nucleophilic addition reactions [25].

In plasma processing, energetic ions incident upon the surface typically provide necessary energy to initiate surface chemical reactions, so that surface modification, film deposition, or surface etching can take place at low surface temperature in non-thermodynamical-equilibrium conditions [26]. Molecular dynamics (MD) simulation for gas-phase ions and atoms interacting with atoms of a solid material can reveal some aspects of such non-equilibrium surface chemical reactions taking place during plasma treatment of polymers at the atomic level [27, 28].

As a practical motivation for the paper, we performed induced pluripotent stem (iPS) cells cultivation on non-treated cultivation polystyrene Petri dish and dishes treated by N_2/H_2 inverter and plasma polymerized cyclopropylamine (CPA). In preliminary experiments, we observed that compared with the control case the inverter plasma-treated dishes and the CPA plasma polymerized dishes help iPS cells retain their multipotency. Although the details of underlying cell-surface interaction remain unclear, the critical part is the selective binding of mediating proteins (albumins) and proteins of extra-cellular matrix to amine groups. The adsorbed proteins effectively create coating with specific ligands required for iPS cells attachment and proliferation [29, 30]. Despite this is merely a qualitative observation, this result suggests that both surfaces modified by plasma processes result in surfaces with sufficient concentration of primary amine groups for cell attachment.

MD simulations were carried out to assess a possible difference between the plasma treatment of polymers aiming to introduce amine groups at the surface and plasma polymerization in the mixture with high potential to produce amine-rich thin films. The simulation initial conditions were chosen to resemble some relevant experiments into which the simulation results could bring more understanding and to which they could be compared. The first case assumed that NH_2 radicals arriving at the surface of polystyrene with near thermal energy together with fast NH_3 molecule having the energy of 100 eV. These conditions can represent some of the best yet realistic situation for the introduction of NH_2 groups onto polystyrene and can be linked to the N_2/H_2 inverter plasma experiment. A highly simplified view on the plasma polymerization with a precursor containing NH_2 groups was obtained by the MD simulations in which cyclopropylamine molecules arrived at the polystyrene surface with near thermal energy together with Ar atoms with low energy of 10 eV. Furthermore, the energy of fast particles in respective simulations was varied to study the effect of bombardment energy. Particularly for CPA/Ar mixtures, this can represent the plasma polymerization in radiofrequency (RF) capacitively coupled plasma (CCP) of various configurations and DC self-bias imposed at the substrate electrode.

2. Outline of molecular dynamics simulations

A classical MD simulation approach based on the integration of Newton's equations of motion was used to obtain some insight into the process of plasma-based amine ion implantation and amine plasma polymerization on a polystyrene substrate. Interactions among atoms were described by multi-body potential functions are essentially the same as those described in reference [27], which extended Stillinger–Weber type interatomic potential functions [31–34] to double and triple bonds and was used for MD studies on various plasma-polymer interactions [27, 35–39]. The details of the potential functions are provided in Supplementary Information (https://stacks.iop.org/PSST/29/105020/mmedia), section 1.

A model of polystyrene, a rectangular box with the base dimensions 2.32 nm by 2.08 nm, was constructed as a substrate for plasma treatment and deposition. The exact lateral dimensions conveniently fit a prebuilt model of polystyrene, which consisted of horizontally aligned spiral polystyrene chains (see figure S2 in supplementary information). The base dimensions
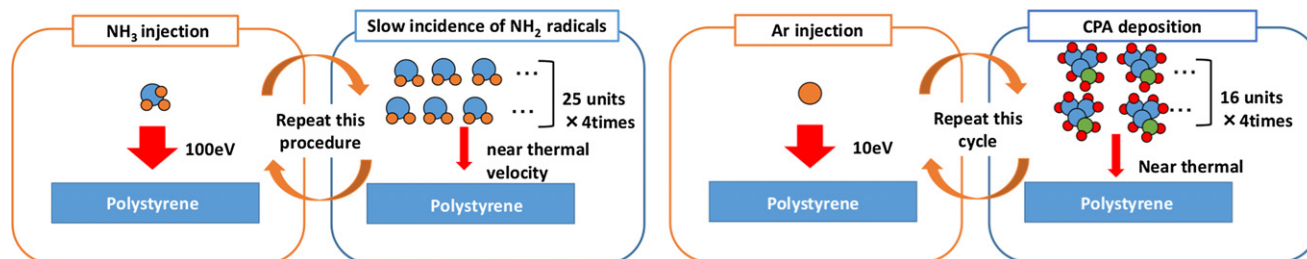
Figure 1. Schemes of the NH$_2$/NH$_3$ (left) and CPA/Ar (right) MD simulations. The model consists of the injection of a fast neutral, either NH$_3$ or Ar, followed by four cycles with the deposition of NH$_2$ radicals or CPA molecules having a near thermal velocity.

of about 2×2 nm and the height of ≈ 11 nm were chosen as a compromise between computational time (number of particles and therefore computational time increases as the product of length and width), the fidelity of simulated polymer properties (which requires long chains) and the depth of energetic particle penetration that should not reach the bottom of the box. The periodic boundaries were imposed to simulate larger surfaces.

Impinging particles were inserted into the simulation with the velocity vector in the direction normal to the surface. All particles were modeled as charge-neutral, assuming the Auger neutralization process for bombarding ions. Each cycle the MD simulation was performed for 2000 fs. For each impact, the simulation was performed in the microcanonical conditions for 1000 fs. Then the system was brought to thermal equilibrium at 300 K by the Langevin and subsequently Berendsen thermostat for 900 and 100 fs, respectively, applied to all particles. Desorbed particles were removed from the system at the end of the microcanonical sub-cycle and at the end of the cycle, so their rescaled velocities do not affect the subsequent simulation. With this artificial cooling and relaxation process, excess heat is removed from the system and makes the system ready for the subsequent energetic particle injection. The thermostat algorithm, however, cannot well reproduce long-term thermal relaxation processes of the surface that ensue for microseconds or even milliseconds after each impact of an energetic particle.

The simulations of plasma treatment and deposition were performed by alternating the insertion of the energetic particle (i.e. NH$_3$ molecule and Ar atom, respectively) and slow neutral particles (i.e. NH$_2$ radicals and CPA molecules, respectively). Each simulation was performed with one selected energy of the energetic particle in order to represent the effect of ion bombardment. In the case of the plasma treatment, the cycle with NH$_3$ molecule injection with the selected energy from interval 50–200 eV was followed by 4 cycles each with the injection of 25 NH$_2$ radicals having near thermal energy of 0.5 eV. Similarly, for the CPA plasma deposition, the cycle with the injection of Ar with the selected energy from interval 10–110 eV was followed by 4 cycles each with the injection of 16 CPA molecules with the near thermal energy of 0.1 eV. The figure 1 visually summarizes typical simulation procedures. All the simulations were run for a total of 2000 cycles. Additionally, simulations without energetic particles were run for both presented models. To achieve the same dose of neutrals,

the number of cycles was reduced to 1600 with otherwise the same conditions.

3. Experimental details

3.1. N$_2$/H$_2$ *plasma treatment in bipolar pulsed DC glow discharge*

The polystyrene dishes (35 mm in diameter) were treated in bipolar pulsed dc glow discharge ignited in N$_2$/H$_2$. The bottom molybdenum electrode, 190 mm in diameter, was connected to the inverter power supply whereas the top aluminum electrode (80 mm) was grounded (figure 2) [40, 41]. The distance between the electrodes was 38 mm. The plasma chamber was pumped by a turbomolecular pump backed by a rotary pump. The pressure during the discharge operation was 250 Pa. The flow rates of N$_2$ and H$_2$ were 13.3 and 5 sccm, respectively. The applied positive and negative voltage pulses had the width of 1 μs and the applied voltages were 1.3 and -1.1 kV, respectively. The repetition frequency was 5 kHz. The samples were treated for 30 min.

3.2. CPA plasma polymerization in capacitively coupled plasma

The CPA plasma polymers (CPA PPs) into the polystyrene dishes and on Si substrates (double-side polished) were prepared in a custom build stainless steel parallel plate reactor similarly as in the previous work of Manakhov *et al*. [42]. The bottom electrode, 420 mm in diameter, was connected via a matching box to an RF generator working at the frequency of 13.56 MHz. The gases were supplied into the chamber through a grounded upper showerhead electrode, 380 mm in diameter. The distance between the electrodes was 55 mm. The bottom electrode with substrates was negatively DC self-biased due to the reactor geometric asymmetry. The reactor was pumped down to $\approx 10^{-4}$ Pa by a turbomolecular pump backed by a rotary pump. The deposition was carried out with the rotary pump only. The leak rate including wall desorption was below 0.1 sccm.

The CPA was polymerized in square pulsed CPA/Ar plasma at the nominal power of 100 W and the pressure of 50 Pa. The pulse duty cycle and repetition frequency were 33% and 500 Hz, respectively. The flow rate of Ar was set to 28 sccm and regulated by an electronic flow controller Hastings, whereas the flow rate of CPA vapors was set to 2 sccm by a needle valve. The substrates were sputter-cleaned by pulsed
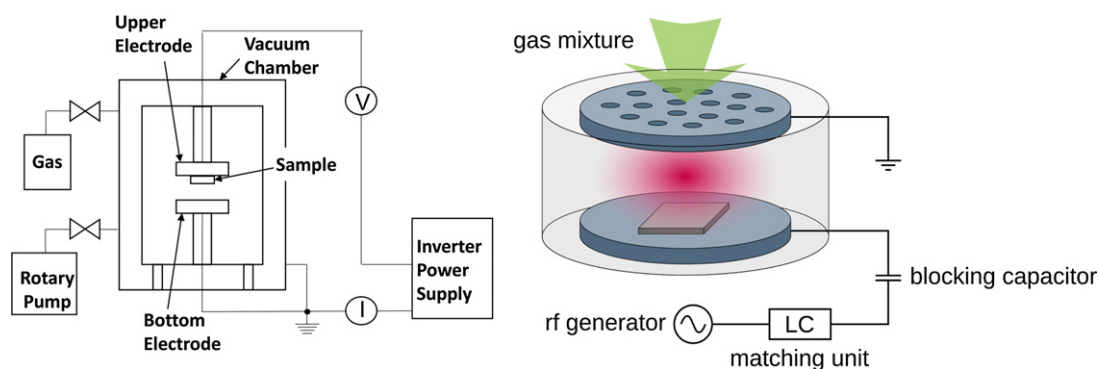
Figure 2. Schemes of the bipolar pulsed DC discharge (left) and capacitively coupled plasma (right) reactors.

Ar plasma for 10 min prior to the deposition. The deposition time was 60 min. The film thickness measured by ellipsometry in the UV-visible range was 249 nm.

3.3. Sample analysis

The quantitative atomic composition (without hydrogen) of the CPA PPs on Si substrate was obtained by monochromatized X-ray photoelectron spectroscopy (XPS) using the Axis Supra spectrometer (Kratos Analytical) at the pass energy of 20 eV. The maximum lateral dimension of the analyzed area was 0.7 mm. A sample differential charging was avoided by a charge neutralization in the overcompensated mode. The depth profiling was performed with Ar cluster gun rastering over a square area with the side dimension of 1.9 mm. Argon clusters with an average size of 500 atoms were accelerated to the energy of 20 keV.

The quantitative atomic compositions of the samples prepared by the N_2/H_2 plasma treatment of the polystyrene were obtained by non-monochromatized XPS ESCA850M (Shimadzu Corporation) using pass energy of 75 eV. The spot diameter was 8 mm. The depth profiling was performed by Ar ion gun with the accelerating voltage of 1 kV.

4. Results and discussion

4.1. Simulation of NH_2/NH_3 surface treatment

The MD simulation performed with slow NH_2 radicals and NH_3 energetic molecules represents one of the best scenarios for the formation of primary amine groups at the polystyrene surface treated in plasma with support of energetic ions. The resulting structures are evaluated after 2000 simulation cycles, which is sufficient to reach a steady-state of presented observable quantities. As an example, we discuss the simulation with the NH_3 energy of 100 eV. Few snapshots of the atomic configurations during simulation can be found in the supplementary information, figure S3. Figure 3 depicts the depth profiles of elements (a) and interatomic bonds in carbon and nitrogen environments (b and c, respectively). The simulation predicts overall slow etching of the original polystyrene surface. Approximately 0.2 carbon atom is removed per impact of energetic particle.

A locally higher concentration of nitrogen than carbon can be noted near the surface in figure 3(a). We will first introduce a naive approach to the calculation of nitrogen content as it would appear by XPS analysis of simulated surfaces and refine it later. Since the nitrogen concentration is not constant, the lower edge of the modified layer was considered as the depth in which the nitrogen intensity reaches half of the maximum. The nitrogen content of the modified layer is calculated only from the volume above the edge of the modified layer. For the comparison with the experimental results, the ratio [N]/([N] + [C]) in the modified/deposited layers is used throughout the text because XPS is not able to detect the hydrogen and [N]/([N] + [C]) ratio is therefore analogous to atomic concentration. In the example given in figure 3, i.e., for the NH_3 energy of 100 eV, the [N]/([N] + [C]) is 0.69 and the thickness of nitrogen-containing mixing layer is about 20 Å.

The depth profiles of chemical bonds in figures 3(b) and (c) show that N–H and C–N bonds are dominant near the top surface, followed by the number density of cross-linking bonds C–C and N–N bonds. The C–H terminating bond of the original polymer is almost not present. The high concentration of C–N bonds reveals that incorporated NH_2 radicals are easily dehydrogenated by other incoming radicals and form new C–N bond with neighboring carbon atoms. The high concentration of relatively weak N–N bonds (hydrazines or diazanes) can be explained by the simultaneous introduction of many NH_2 radicals. During the impact, NH_2 radicals readily form hydrazine (N_2H_4) which is incorporated into the surface. This is further supported by CPA/Ar simulations where N–N bonds are practically not present.

The highly cross-linked nature of mixing surface layer is highlighted by low hydrogen content of 44%, significantly lower than the estimate for the CPA simulations even at the highest argon atom energy. Based on the nitrogen environment shown in figure 3(c), two sublayers can be roughly distinguished in the nitrogen-rich layer: a highly cross-linked C–N rich sublayer close to the surface, and an N–H rich sublayer closer to the bulk polystyrene. Since the stopping distance of particles with the energy of 100 eV is just a few atomic layers [43], the majority of its energy is released in the topmost layer, causing surface mixing and cross-linking, while deeper layers are relatively unaffected. The evaluation of amine groups in the whole volume gives the content of primary amines of 30%, secondary 39% and tertiary 31%. If we focus only on the top C–N rich sublayer, the relative concentrations shift towards more cross-linked (primary amines is 23%, secondary
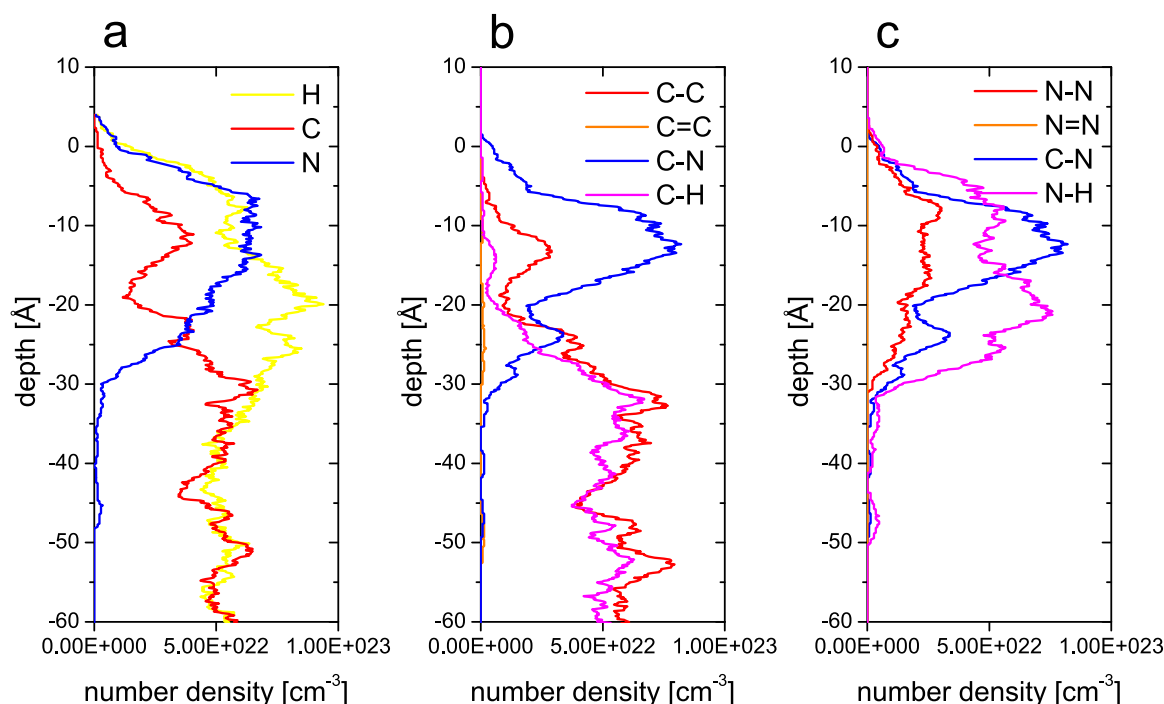
Figure 3. MD simulation results of polystyrene surface treated by NH_2 radicals and energetic NH_3 molecules (100 eV). Figures present (a) depth profiles of elements, (b) different carbon and (c) nitrogen bonds. The depth is given relative to the original polystyrene surface.

42% and tertiary 35%) showing that primary amine groups are preferentially buried deeper as suggested in the previous paragraph. Further analysis also shows the formation of some nitriles (triple bonded $C \equiv N$), which are not present in CPA/Ar simulations.

The reflected and etched species are dominated by non-sticking NH_2 radicals and volatile products such as N_2H_4 and NH_3. Further, less abundant species produced by surface reactions are H_2, N_2, CN and CNH. There is no prevalent channel of carbon removal from the original polystyrene surface. Various small molecules (e.g., C_2H_2, CN or CNH), and even some large ones (typically $C_{5+}N_{10+}H_{15+}$) contribute to etching.

4.2. Simulation of CPA/Ar plasma deposition

Unlike in high voltage N_2/H_2 and NH_3 plasma treatment [2], the plasma polymerization is performed under much milder energetic conditions because the functional groups of the monomer should be retained as much as possible [20]. Therefore, the MD simulation of CPA/Ar with the Ar atom energy of 10 eV was chosen as a typical example for the discussion of the process in this section. Few snapshots of the atomic configurations during the simulation can be found in the supplementary information, figure S4.

The film composition profiles (elements and chemical bonds) obtained from the MD simulation are shown in figure 4. Even at such low energy, the nitrogen concentration extends below the original substrate-level due to partial etching of polystyrene and the creation of the mixing layer. This effect is even more pronounced for higher energies as discussed below.

It should be noted that, besides Ar kinetic energy, effectively also internal potential energy is introduced with each CPA molecule. Due to high internal bond stress, the CPA carbon ring is prone to relax by ring-opening and formation of a radical. Thus, each CPA molecule brings ≈ 6.5 eV of internal energy. It can be considered as plasma activation, which is in fact required as non-radical CPA neutrals would have very low sticking probability.

The MD simulation predicts slow deposition of nitrogen-containing thin film, with relatively constant concentration profiles. Only about one carbon or nitrogen atom is on average deposited per CPA cycle, i.e., per 64 CPA molecules. The resulting thin film is significantly different from layer predicted in NH_2/NH_3 simulation in both the elemental composition and chemistry. The simulated nitrogen concentration captured by the ratio $[N]/([N] + [C])$ of 0.18 is only about one third of the value for NH_2/NH_3. Compared to the NH_2/NH_3 simulation, the CPA film is also more hydrogenated ($[H] > 0.53$).

As expected from elemental composition, the bond profiles show that dominant bonds are terminating C–H, followed by cross-linking C–C and C–N bond. In the nitrogen environment, the concentration of N–H bonds is significantly lower than cross-linking C–N bonds. It suggests that the majority of nitrogen forms secondary or tertiary amines.

The species reflected and sputtered from the surface during the deposition are volatile and non-sticking products of surface reactions. Interestingly, the most prominent fragment is not CPA (C_3NH_7) reflected from the surface but C_2NH_5 fragment, followed in abundance by NH_2, C_3H_5 and then C_3NH_7. All these fragments smaller then CPA are products of single dissociation of linear C_3NH_7. Fragments larger than the original molecule are also present, however, with a lower relative
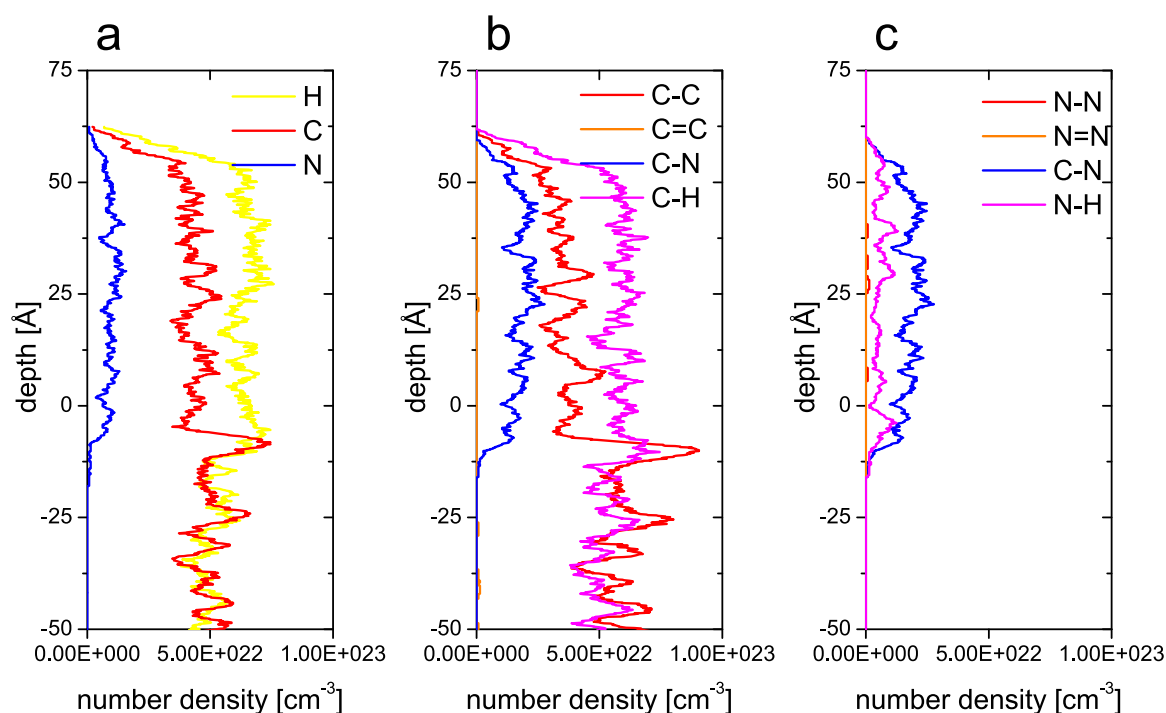
Figure 4. Depth profiles of simulated CPA plasma polymer layer for Ar energy of 10 eV. Figures present (a) depth profiles of elements, (b) different carbon and (c) nitrogen bonds. The depth is given relative to the original polystyrene surface.
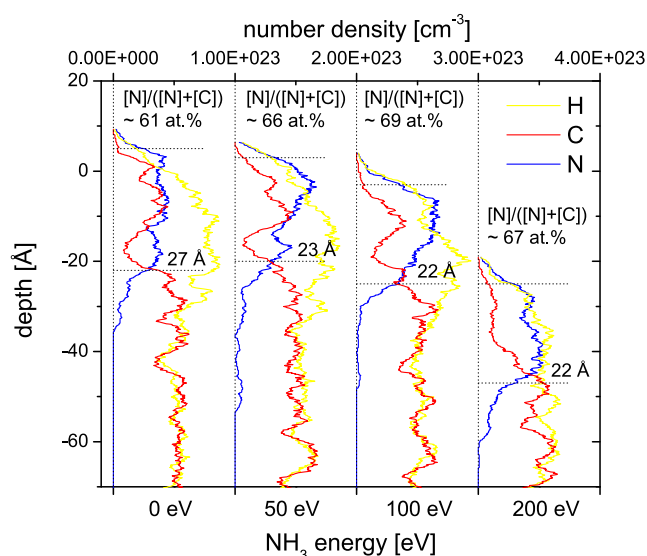

Figure 5. The composition profiles resulting from NH_2/NH_3 simulations with the NH_3 energy of 0, 50, 100 and 200 eV. The steady-state thickness of the nitrogen-rich layer and the nitrogen concentration is depicted for each simulation. The depth is given relative to the original polystyrene surface.

abundance which is significantly decreasing with the fragment mass.

4.3. Effect of particle energy in MD simulations

To study further the effect of ion bombardment on the plasma treatment and deposition we run series of simulations with varying energy of fast NH_3 molecule and Ar atom, respectively.

4.3.1. NH_2/NH_3 surface treatment. As demonstrated by the elemental composition profiles in figure 5, a nitrogen-rich mixing layer is formed for all the tested NH_3 energies, even if the energy is set to zero. The nitrogen-rich layer has the steady-state thickness of 20 Å being almost unaffected by the energy of NH_3 molecule. The profiles simulated with 50 eV NH_3 are similar to the results with 0 eV. The polystyrene etching becomes noticeable for 100 eV and it is clearly pronounced for 200 eV. The nitrogen content $[N]/([N] + [C])$, also given in figure 5, is similar for all tested energies except 0 eV simulation, that resulted in a lower value of 0.61. The values of $[N]/([N] + [C])$ appear unrealistically high when compared to the surface analysis of experimental samples but the simulated values need some corrections as discussed in section 4.4.

The density of the nitrogen-rich layer formed in the polystyrene (figure 6(a)) exhibits a maximum at 100 eV of NH_3 and then decreases for the highest energy of 200 eV. We assume that sputtering effects at 200 eV result in fast removal of material from the surface. Even though the energy and momentum are higher in the 200 eV case, the residence time in the surface volume is significantly shortened and overall physical densification by energetic bombardment is, therefore, lower than for the lower bombardment energy. At the same time, the chemical effects of energetic bombardment show simple trends even for the highest energy (figure 6). The content of hydrogen, the relative amount of terminating N–H bonds and weak N–N bonds are decreasing with the NH_3 energy, while the relative amount of strong cross-linking C–N bonds in the nitrogen environment increases.

Figure 7 shows the effect of ion bombardment on the relative concentrations of different amine groups. The content of primary amines of 52% is obtained in the simulation without
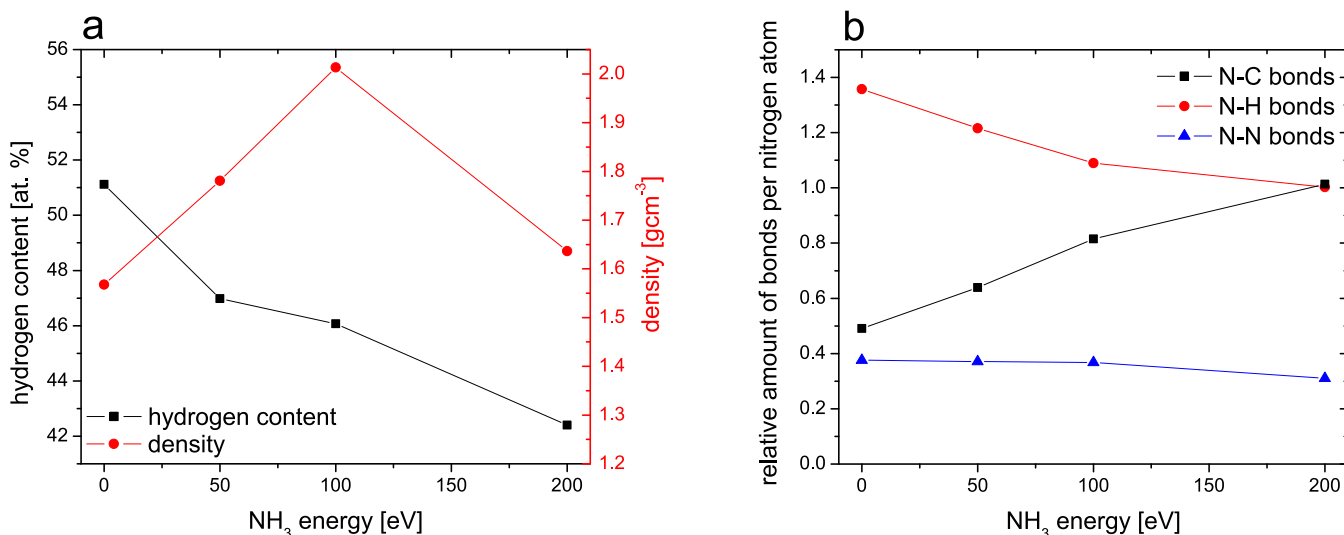
Figure 6. Properties of simulated nitrogen-rich layers in polystyrene treated by NH_3/NH_2 in dependence on NH_3 energy: (a) hydrogen concentration and density, and (b) nitrogen chemical environment.
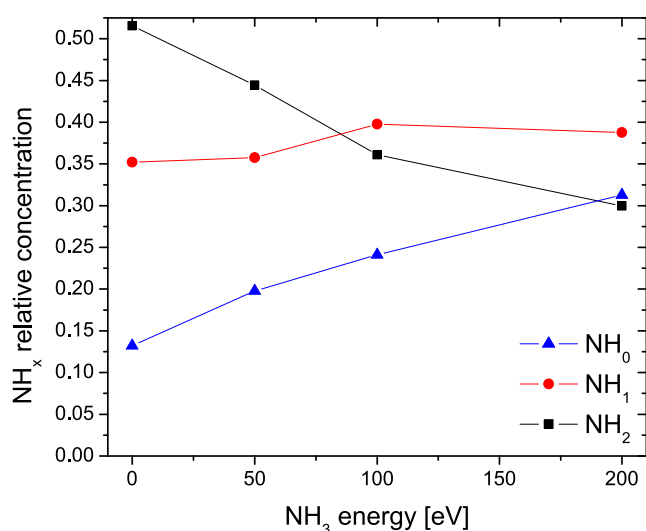

Figure 7. Relative concentrations of primary (NH_2), secondary (NH_1) and tertiary amines (NH_0) in NH_2/NH_3 simulations.

Figure 8. Number of selected species desorbed from the surface during energetic NH_3 cycles in the NH_2/NH_3 simulations.

energetic bombardment. Although such simulation represents an almost ideal case for the functionalization of polystyrene by primary amine groups, the surface reactions initiated by the NH_2 radicals are sufficient to reduce the primary amine specificity to approximately a half. The content of primary amines is decreasing with the NH_3 energy down to $\approx 30\%$. Secondary amines exhibit quite stable concentration at $\approx 35\%$, slightly increasing to $\approx 40\%$ for the higher energies. The concentration of highly cross-linked tertiary amines is increasing from 13% to 25% with the NH_3 bombardment energy.

We show products of energetic bombardment by NH_3 in figure 8 depicting number of selected species desorbed or sputtered from the surface during the total of 400 energetic NH_3 cycles. Populations of all the species are increasing with the energy of incident NH_3 molecule. The high number of NH_2 and N_2H_4 even for the lowest energy of 50 eV suggest that these species remain weakly attached to the surface
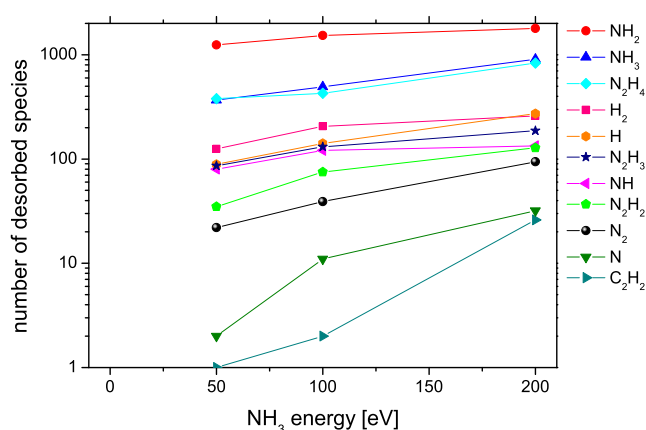
from the previous cycles and are readily removed even by relatively low energy bombardment. The figure also highlights C_2H_2 molecule as the main channel for carbon etching by high energy bombardment.

4.3.2. CPA/Ar plasma deposition. Figure 9 shows that the deposition rate decreases with the energy of Ar atom in CPA/Ar simulation. It suggests that the internal energy of CPA is sufficient for radical formation and promotion of sticking probability even without a surface activation by energetic particles. Increasing energy of Ar atom causes a gradual decrease of the deposition rate which is becoming significantly steeper for the energy of 50 eV and higher. Unlike metals, polymers do not show a threshold energy for sputtering. A variety of physical and chemical effects is induced by particle bombardment, including both atomic and molecular motion regimes of collision cascade inside a polymer chain and collisional mixing [44]. In principle, any particle with kinetic energy higher than the dissociation energy is able to release fragments from the surface, although with a very low probability for small
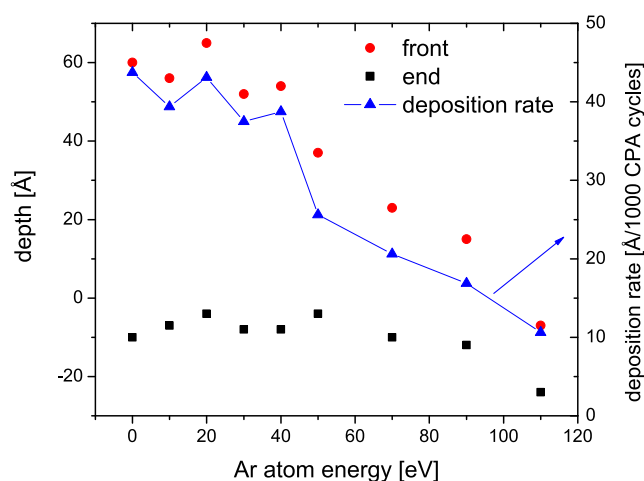
Figure 9. The position of the CPA-film top and bottom surfaces with respect to the surface of the original polystyrene substrate in the dependence on the Ar atom energy as obtained from the MD simulations. The dependence of the resulting CPA-film deposition rate on the Ar atom energy is shown on the right *y*-axis.

Figure 10. Nitrogen concentration in CPA plasma polymer as simulated by molecular dynamics. Linear fit is added as a guide to the eye.

energies. The physical sputtering of polymers by very low energy argon ions (<100 eV) was not studied in detail to our knowledge. However, extrapolating from limited published data, sputtering of the polymer can become significant at this energy [45].

The simulated nitrogen content [N]/([N] + [C]) for higher energies of Ar atom is shown in figure 10. Surprisingly, we observe an increasing trend with argon energy. The data points at higher energies have worse statistics as there is a slower deposition rate and, therefore, a lower number of film particles in the simulation. However, this effect cannot account for the increasing trend. In a highly cross-linked material subjected to energetic bombardment, nitrogen could be considered more volatile than carbon, as it has one bond less. Since the simulated films are still far from fully cross-linked (with about 50% of hydrogen), we conjecture that some geometrical effect of CPA dissociation might be responsible for preferential carbon removal. We further discussed the increasing trend of nitrogen concentration with energy in section 4.4.

The increasing cross-linking of simulated CPA thin films with Ar energy is reflected in the concentration of hydrogen and thin film density shown in figure 11(a). Since hydrogen cannot participate in the chain propagation its concentration can be used as a rule of the thumb for polymer cross-linking [46]. The decrease in hydrogen content and densification by bombardment is reflected also by the calculated density shown in the figure right axis. The simulated densities increase from 1.17 to 1.57 g cm^{-3} with increasing bombardment energy, consistently with both, the experiment and theory [47]. The trend in cross-linking is further supported by figure 11(b) showing an increasing ratio of C–N bonds in the nitrogen environment.

Further analysis of different amine groups in figure 12 reveals that their relative concentrations are relatively stable, particularly for the lower energy of Ar atom. The relative content of primary amines is lower than in the case of NH$_2$/NH$_3$ simulations. Even without energetic bombardment (0 eV), it is limited to 21% and remains similar for low bombardment
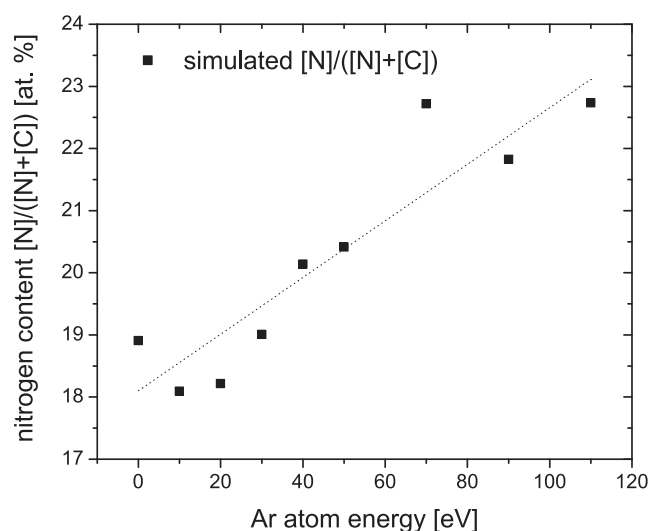
energy (<50 eV). Finally, for the energy of 50 eV and higher, the relative content of primary amines decreases to $\approx 16\%$. The relative content of secondary amines is $\approx 35\%$. The concentration of highly cross-linked tertiary amines is increasing with bombardment energy, from $\approx 40\%$ to $\approx 50\%$. Since primary and secondary amines contain both C–N and N–H bonds, the effect of bombardment (figure 11(b)) almost cancels out, yielding a relatively stable concentration, while tertiary amines formed by C–N bonds increase with the Ar energy. Thus the analysis reveals that even though ion bombardment has a significant effect on thin film deposition rate, cross-linking and densification, the impact onto the chemistry is rather limited. We hypothesize that once the surface is given sufficient energy the system tends to stabilize at a state with minimum energy, that is likely the chemistry with a lower content of primary amines. Moreover, in the experiment, the lower accessibility of primary amines due to increased cross-linking and densification can further contribute to a lower detected concentration of primary amines for higher power and bombardment energy conditions [48].

Comparing populations of species desorbed or sputtered during the energetic Ar cycles (total of 400) in figure 13 gives further hints on bombardment effects on the surface. The majority of species with a high abundance are products of CPA dissociation (C$_2$NH$_5$, C$_3$H$_5$, NH$_2$, CH$_3$) and CPA itself (C$_3$NH$_7$). Populations of all these are largely unaffected by bombardment and are removed even by Ar bombardment with the lowest energy of 10 eV, suggesting that they are only loosely bonded to the surface and might be eventually released even without bombardment. Contrary, some small molecules (H, H$_2$, C$_2$H$_2$ and C$_2$H$_2$) exhibit clear increasing trend with Ar bombardment energy, implying that they are sputtered by the bombardment. Note that this sputtering is preferential to carbon, as the nitrogen-containing species do not display on average such strong dependence to Ar energy. We assume, the preferential sputtering is a geometrical effect is caused by dissociation and bonding pattern of CPA molecule.
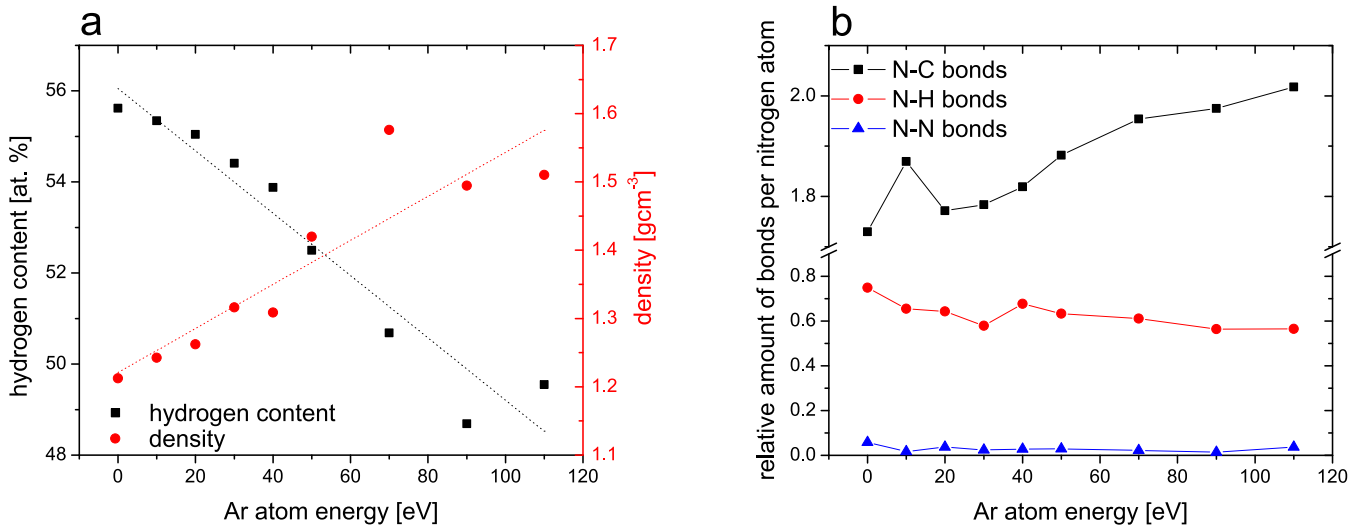
Figure 11. Concentration of hydrogen and density of simulated CPA thin film in dependence on energy of argon atom (a) and simulated nitrogen environment in CPA plasma polymer deposition (b). In plot a, linear fits are added as a guide to the eye.
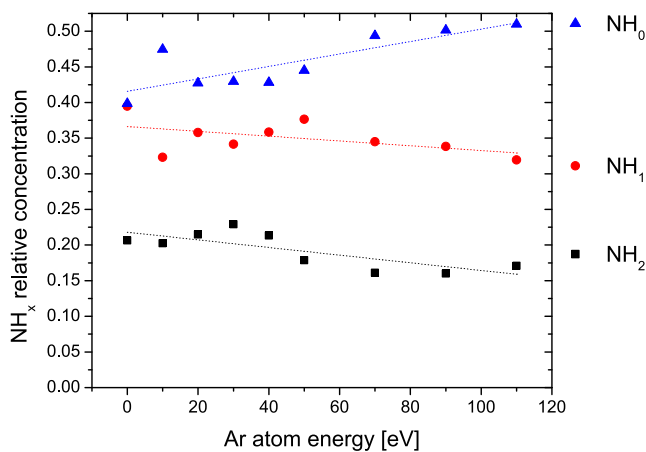

Figure 12. Relative concentrations of primary (NH_2), secondary (NH_1) and tertiary amines (NH_0) in CPA/Ar simulations. Linear fits are added as a guide to the eye.
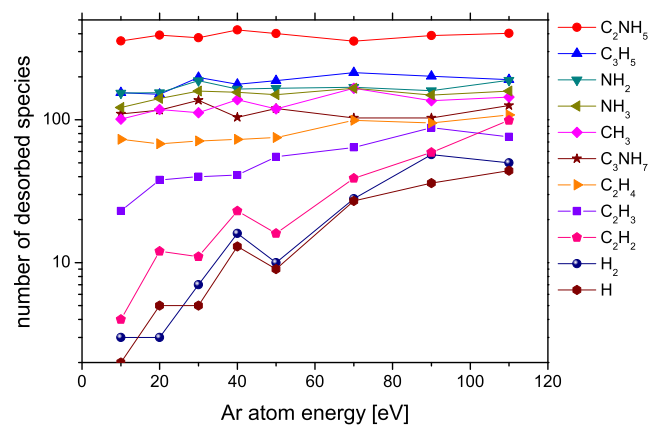

Figure 13. Number of selected species desorbed from the surface during energetic Ar cycles in the CPA/Ar simulations.

4.4. Discussion on comparison with experiments

4.4.1. Agreement between the simulations and XPS experimental results. The MD simulation conditions described above are extremely simplified models of real plasma processes that involve many more species and ion energy distributions. We designed the simulations to highlight the effect of ion bombardment in conditions otherwise favorable for the formation of primary amine groups. Other problems that can hinder the agreement between the simulation and experimental results are related to limitations inherent to molecular dynamics, (i) the discrepancy between the spatial and temporal scales accessible by the MD simulation and the experiment and (ii) the precision of potential functions, particularly for slow processes and reactions. Although the simulations are not necessarily predictive for the respective experiments [28], we show in the following paragraphs that the agreement with our experiments can be reasonably good if we take into account the experimental and simulation limitations.

Some observables readily accessible in the simulations, e.g., the concentration of hydrogen, are difficult to measure experimentally. We focused mainly on the XPS measurements of nitrogen, primary amines, and the XPS depth profiling of nitrogen. To compare the measured XPS and the simulated depth profiles, we calculated 'synthetic' XPS depth profiles from the simulated data by taking into account an inhomogeneity of the elemental concentration. We used the simplest approach assuming that photoelectrons are only lost due to inelastic collisions. Then, the concentration of element A, [A], is proportional to the integral of its number density $N_A(z)$ multiplied by the exponential depth decay:

$$[A] \propto \int_0^\infty N_A(z) \, \exp\left(-\frac{z}{\lambda_i}\right) \, dz. \tag{1}$$

where λ_i is the inelastic mean free path estimated for typical nitrogen-containing polymers as 30 Å [49]. Applying equation (1), we can calculate the effective nitrogen concentration $[N]/([N] + [C])|_{\mathrm{sim\,xps}}$ that would be determined by XPS on the surfaces created by the simulation. The $[N]/([N] +$

[C])|$_\mathrm{sim\,xps}$ evaluated after the simulation with the flux of NH$_2$ radicals and NH$_3$ energetic species is much lower than the nitrogen concentration naively estimated in sections 4.1. and 4.3.1 without considering the depth concentration inhomogeneity in which the nitrogen-rich layer is only about 20 Å, i.e., lower than the XPS information depth.

The XPS nitrogen concentration [N]/([N] + [C])|$_\mathrm{sim\,xps}$ calculated with the help of equation (1) is 0.48 instead of 0.69 reported in section 4.1 for the simulation with 100 eV NH$_3$ species. It is still much larger than our experimental value 0.25 obtained after N$_2$/H$_2$ plasma treatment. The experimental XPS nitrogen concentrations [N]/([N]+[C] reported for plasma treatment experiments are usually even lower than 0.25 [50–53]. The simulated values [N]/([N] + [C])|$_\mathrm{sim\,xps}$ are therefore clearly exaggerated. We assume that it is caused by shortcomings typical for molecular dynamics. The time scales during which high fluxes of particles are impacting the surfaces are only few nanoseconds in our simulations. Therefore, the simulation do not account well for slow processes such as thermal desorption of weakly bonded fragments, surface reorganization, or slow chemical reactions in general. Secondly, the potential function was optimized on a set of stable chemical compounds and its application to the functionalization of a surface by radicals might stretch it beyond its applicability.

Species in the NH$_2$/NH$_3$ simulation were selected to facilitate favorable conditions for the formation of primary amine groups. However, the real plasma-chemical processes in the N$_2$/H$_2$ plasma treatment experiment are expected to provide only moderate amount of NH$_2$ radicals [54, 55]. In this regard, simulation might correspond better to NH$_3$ discharges. Moreover, the formation of primary amine groups in the surface was shown to be a more complicated process, likely involving also other NH$_x$ radicals, atomic nitrogen and hydrogen [3, 17]. Energy and relative dose of energetic particle bombardment were chosen close to estimates for the given discharge and pressure [56, 57].

The experimental conditions of CPA plasma polymerization suggest that the ion energy involved in the process is quite low, definitively much lower than in the case of N$_2$/H$_2$ inverter plasma experiment and related MD simulations. We estimated that typical ion energy representing the CPA PP experiment is 10 eV [42, 47]. The predicted elemental composition results for 10 eV Ar, captured by the ratio [N]/([N] + [C])|$_\mathrm{sim\,xps}$ of 0.16, agrees very well with the experimental XPS (also 0.16).

The predicted trend of increasing nitrogen incorporation with energetic particle energy, shown in figure 10, is opposite to our previous experimental findings. In the case of CPA/Ar deposition, we have observed a decrease of N/C within range 0.23–0.12 with the radio-frequency power [42] that is linked, in the capacitively coupled discharges, to higher mean ion energy. The disagreement between the simulated trend in N/C and the experimental results can be, to a certain degree, attributed to a decreased statistical significance in the simulation results because of decreased number of deposited particles for higher energy of particles. However, we assume that the main factor is a change of the gas phase composition when higher RF power is applied. For low ion energy (and

therefore power), the plasma polymerization process is still in the energy deficient regime, with relatively similar dissociation pattern. For a higher power and the monomer deficient regime, the gas phase composition in the experiment can change quite significantly. Secondly, as we already noted for NH$_2$/NH$_3$ simulations, our simulations poorly predict the balance between sticking and desorption of nitrogen-containing radicals, which are more likely to form in simulations with a higher energy of argon atoms.

The experimental concentration of primary amines [NH$_2$]/[N] reported for NH$_3$ discharges varies widely based on the treatment type. In paper of Favia *et al*, the direct treatment in RF CCP yielded moderate value of 16%, while afterglow of the same discharge resulted in [NH$_2$]/[N] up to 70% [3], possibly highlighting the role of ion bombardment. Also other authors were able to achieve high amine specificity, with [NH$_2$]/[N] up to 100%, however, only by employing remote or downstream plasma [58, 59]. Our simulations NH$_2$/NH$_3$ simulations show qualitative agreement with the reported results, with [NH$_2$]/[N] of 52% in condition without bombardment (0 eV) and decreasing to 30% for the highest NH$_3$ energy. The experimental concentration of primary amines [NH$_2$]/[N] ≈ 9% was reported for the CPA/Ar discharge [48]. This value is about half of the concentration in the CPA/Ar simulation [NH$_2$]/[N] of 16%–22%. Yet, the simulation should be considered as the upper limit estimate, as it cannot account for thermal desorption, slow chemical reactions and aging in the ambient atmosphere, which can decrease the primary amine concentration in the experiment.

4.4.2. Composition profiles. We present a comparison of the experimental two plasma modified surfaces by XPS depth profiling in figure 14(a). The concentrations of nitrogen [N]/([N] + [C]) at the top surfaces are comparable. A higher nitrogen concentration of 0.25 is detected for N$_2$/H$_2$ plasma-treated surface. The concentration, however, sharply decreases and already at depth of 20 Å is ≈0.04. Note that this depth profiling was done by energetic Ar ion beam which is known to cause surface mixing and preferential sputtering [60]. Therefore, the non-zero concentration in larger depths can be attributed to the mixing effect. The surface of plasma polymerized CPA shows [N]/([N] + [C]) of ≈0.16 which slightly increases with depth to a steady-state value of ≈0.17 throughout the thickness of thin film.

It is well recognized that plasma treatment leads to the functionalization of a very thin near-surface layer usually with a short life-time [18]. On the other hand, the deposition of amine containing coating creates a relatively thick layer that does not have a strong chemical gradient at the surface and therefore does not suffer from surface reorganization. By this approach the stability of amine groups can be enhanced and, thus, the aging effect reduced [1].

From the simulated elemental profiles, we can also calculate the simulated XPS profile by evaluating intensity as function integral upper limit in equation (1). For simplicity we do not consider any mixing by sputtering, the simulated XPS profiles are shown in figure 14(b).
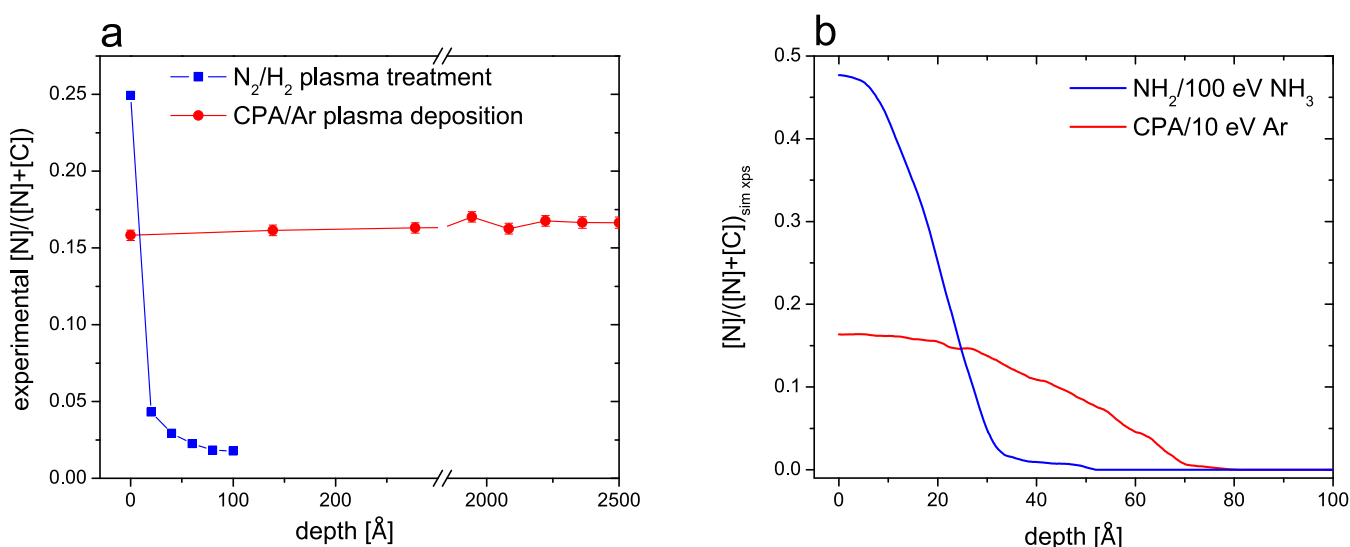
Figure 14. The experimental XPS depth profiles of samples created by plasma treatment in DC bipolar pulsed discharge and CPA/Ar plasma polymerization in RF capacitively coupled discharge are compared in figure (a). The simulated XPS profiles based on the MD simulation results of elemental density profiles are given in figure (b).

For NH_2/NH_3 simulation, apart from the non-physically high nitrogen concentration, we can still compare the decrease of nitrogen concentration with depth with the experiment. The depth for which $[N]/([N] + [C])|_{sim\,xps}$ drops to half of the maximum value is about 25 Å, which agrees well with experimental XPS depth profiling and estimates acquired for similar experiments by angle-resolved XPS in literature [61, 62]. In CPA/Ar simulation, the thickness of the deposited layer is comparable with the XPS information depth and therefore we do not observe plateau as in the experiment.

5. Conclusion

We have presented results of molecular dynamics simulations of the plasma treatment of polystyrene by the flux of NH_2 radicals combined with NH_3 energetic bombardment and the plasma polymerization of CPA under Ar energetic bombardment. The conditions used for the simulations represent the best possible scenario for the polystyrene surface functionalization by plasma treatment. It is shown that increased energy of NH_3 molecules decreases the retention of primary amines from 52% for 0 eV to 30% for 200 eV. The plasma treatment naturally tends to a more stable state, a low content of primary amines, provided there is a sufficient energy delivered through energy flux. The treatment at any NH_3 energy formed nitrogen-rich layer with the thickness of about 20 Å due to an equilibrium between the modification of top surface and its removal by etching. In the case of CPA plasma polymerization the thickness of the deposited film decreases with the Ar energy above 50 eV. The nitrogen content in the film increases with the Ar energy but it is not related to the increase of primary amine groups. The higher energy flux leads to higher cross-linking of the films as demonstrated by a decrease of hydrogen content and an increase of the film density. However, the impact onto the chemistry is rather limited. The content of primary amines is lower than in the case of plasma treatment

by NH_2/NH_3, 21% for 0 eV energy of Ar and about 16% for the energy of 50 eV or higher.

The results of simulations were compared with the XPS analysis of polystyrene samples prepared in N_2/H_2 bipolar pulsed discharge and coated by plasma polymer thin film deposited in CPA/Ar capacitively coupled RF discharge. The simulation results, especially for the plasma treatment producing only 20 Å nitrogen-rich layer and for very thin CPA plasma polymer films deposited at high Ar energy, had to be recalculated taking into account the information depth of the XPS method. After the correction, the simulated XPS atomic concentration of nitrogen was lower but yet the values for NH_2/NH_3 conditions (0.48 at 100 eV NH_3 assumed as a typical ion energy in the bipolar pulsed discharge) were too high to correspond to our or any other experimental values (below 0.22). It is explained by shortcomings typical for molecular dynamics—only a very short time scale processes accessible in the simulations and a particular selection of the interaction potential function optimized on a set of stable chemical compounds. The agreement for the CPA/Ar plasma polymerization was much better concerning the value of the nitrogen concentration (0.16 for 10 eV Ar assumed as a typical ion energy in the CPA/Ar RF discharge at 50 Pa). However, the predicted trend of increasing nitrogen concentration with Ar energy was opposite to the decreasing trend obtained in the experiments carried out with increased RF power, i.e., increased DC self-bias. It reveals that enhanced gas-phase dissociation of CPA molecules at higher RF power is much more important than the effect of ion bombardment.

ORCID iDs

Miroslav Michlíček ⓘ https://orcid.org/0000-0001-6901-7466

Satoshi Hamaguchi ⓘ https://orcid.org/0000-0001-6580-8797

Lenka Zajíčková ⓘ https://orcid.org/0000-0002-6906-8906

References

[1] Siow K S, Britcher L, Kumar S and Griesser H J 2006 *Plasma Process. Polym.* **3** 392–418

[2] Arefi-Khonsari F, Kurdi J, Tatoulian M and Amouroux J 2001 *Surf. Coat. Technol.* **142–144** 437–48 Proceedings of the 7th International Conference on Plasma Surface Engineering

[3] Favia P, Stendardo M V and d'Agostino R 1996 *Plasma Polym.* **1** 91–112

[4] Girard-Lauriault P-L, Desjardins P, Unger W E S, Lippitz A and Wertheimer M R 2008 *Plasma Process. Polym.* **5** 631–44

[5] Ruiz J-C, St-Georges-Robillard A, Thérésy C, Lerouge S and Wertheimer M R 2010 *Plasma Process. Polym.* **7** 737–53

[6] Hegemann D, Hanselmann B, Guimond S, Fortunato G, Giraud M-N and Guex A G 2014 *Surf. Coat. Technol.* **255** 90–5

[7] Müller M and Oehr C 1999 *Surf. Coat. Technol.* **116–119** 802–7

[8] Choukourov A, Biederman H, Slavinska D, Hanley L, Grinevich A, Boldyryeva H and Mackova A 2005 *J. Phys. Chem. B* **109** 23086–95

[9] Finke B, Schröder K and Ohl A 2009 *Plasma Process. Polym.* **6** S70–4

[10] Abbas A, Vivien C, Bocquet B, Guillochon D and Supiot P 2009 *Plasma Process. Polym.* **6** 593–604

[11] Jarvis K L and Majewski P 2013 *Plasma Process. Polym.* **10** 619–26

[12] Nakamura R, Muguruma H, Ikebukuro K, Sasaki S, Nagata R, Karube I and Pedersen H 1997 *Anal. Chem.* **69** 4649–52

[13] Biederman H, Boyaci I H, Bilkova P, Slavinska D, Mutlu S, Zemek J, Trchova M, Klimovic J and Mutlu M 2001 *J. Appl. Polym. Sci.* **81** 1341–52

[14] Creatore M, Cicala G, Favia P, Lamendola R and d'Agostno R 1998 *MRS Proc.* **544** 115

[15] Lachmann K, Michel B and Klages C-P 2009 *Plasma Process. Polym.* **6** S401–5

[16] Klages C-P, Hinze A, Willich P and Thomas M 2010 *J. Adhes. Sci. Technol.* **24** 1167–80

[17] Klages C-P and Grishin A 2008 *Plasma Process. Polym.* **5** 368–76

[18] Chatelier R C, Xie X, Gengenbach T R and Griesser H J 1995 *Langmuir* **11** 2576–84

[19] Manakhov A, Zajíčková L, Eliáš M, Čechal J, Polčák J, Hnilica J, Bittnerová Š and Nečas D 2014 *Plasma Process. Polym.* **11** 532–44

[20] Ryssy J, Prioste-Amaral E, Assuncao D F N, Rogers N, Kirby G T S, Smith L E and Michelmore A 2016 *Phys. Chem. Chem. Phys.* **18** 4496–504

[21] Saboohi S, Coad B R, Griesser H J, Michelmore A and Short R D 2017 *Phys. Chem. Chem. Phys.* **19** 5637–46

[22] Truica-Marasescu F and Wertheimer M R 2008 *Plasma Process. Polym.* **5** 44–57

[23] Laurent D, Philippe M, Yoann O, Thomas G, Roberto L, Michel H, Jérôme C and Rony S 2010 *Plasma Process. Polym.* **7** 172–81

[24] Daunton C, Smith L E, Whittle J D, Short R D, Steele D A and Michelmore A 2015 *Plasma Process. Polym.* **12** 817–26

[25] Klages C-P and Kotula S 2016 *Plasma Process. Polym.* **13** 1213–23

[26] Oehrlein G S and Hamaguchi S 2018 *Plasma Sources Sci. Technol.* **27** 023001

[27] Yamada H and Hamaguchi S 2004 *J. Appl. Phys.* **96** 6147–52

[28] Graves D B and Brault P 2009 *J. Phys. D: Appl. Phys.* **42** 194011

[29] Lambshead J W, Meagher L, O'Brien C and Laslett A L 2013 *Cell Regen.* **2** 1341–52

[30] Mahlstedt M M, Anderson D, Sharp J S, McGilvray R, Barbadillo Muñz M D, Buttery L D, Alexander M R, Rose F R A J and Denning C 2010 *Biotechnol. Bioeng.* **105** 130–40

[31] Stillinger F H and Weber T A 1985 *Phys. Rev. B* **31** 5262–71

[32] Weber T A and Stillinger F H 1990 *J. Chem. Phys.* **92** 6239–45

[33] Ohta H and Hamaguchi S 2001 *J. Chem. Phys.* **115** 6679–90

[34] Ohta H and Hamaguchi S 2001 *J. Vac. Sci. Technol.* **18** 2373–281

[35] Yamada H and Hamaguchi S 2005 *Plasma Phys. Control. Fusion* **47** A11–8

[36] Yamashiro M, Yamada H and Hamaguchi S 2007 *J. Appl. Phys.* **101** 046108

[37] Yamashiro M, Yamada H and Hamaguchi S 2007 *Jpn. J. Appl. Phys.* **46** 1692–9

[38] Yamashiro M, Yamada H and Hamaguchi S 2008 *Thin Solid Films* **516** 3449–53

Yamashiro M, Yamada H and Hamaguchi S 2008 *Proc. of the Int. Symp. on Dry Process (DPS 2006)* (Nagoya, Japan, November 29–30 2006)

[39] Murakami Y, Horiguchi S and Hamaguchi S 2010 *Phys. Rev. E* **81** 041602

[40] Sugimoto S, Kiuchi M, Takechi S, Tanaka K and Goto S 2001 *Surf. Coat. Technol.* **136** 65–8 Proceedings of the Fifth International Conference on Plasma-Based Ion Implantation

[41] Takechi S, Sugimoto S, Kiuchi M, Tanaka K and Goto S 2001 *Surf. Coat. Technol.* **136** 69–72 Proceedings of the Fifth International Conference on Plasma-Based Ion Implantation

[42] Manakhov A, Landová M, Medalová J, Michlíček M, Polčák J, Nečas D and Zajíčková L 2017 *Plasma Process. Polym.* **14** 1600123

[43] Barton D, Bradley J W, Gibson K J, Steele D A and Short R D 2000 *J. Phys. Chem. B* **104** 7150–3

[44] Delcorte A, Bertrand P and Garrison B J 2001 *J. Phys. Chem. B* **105** 9474–86

[45] Kurihara K, Egami A and Nakamura M 2005 *J. Appl. Phys.* **98** 084907

[46] Denis L *et al* 2011 *Prog. Org. Coat.* **70** 134–41

[47] Hegemann D, Körner E, Blanchard N, Drabik M and Guimond S 2012 *Appl. Phys. Lett.* **101** 3–6

[48] Manakhov A, Michlíček M, Felten A, Pireaux J-J, Nečas D and Zajíčková L 2017 *Appl. Surf. Sci.* **394** 578–85

[49] Cumpson P J 2001 *Surf. Interface Anal.* **31** 23–34

[50] Paynter R W 2000 *Surf. Interface Anal.* **29** 56–64

[51] Wang M-J, Chang Y-I and Poncin-Epaillard F 2003 *Langmuir* **19** 8325–30

[52] Lopez L C, Belviso M R, Gristina R, Nardulli M, d'Agostino R and Favia P 2007 *Plasma Process. Polym.* **4** S402−5

[53] Kleinhans C, Barz J, Wurster S, Willig M, Oehr C, Müller M, Walles H, Hirth T and Kluger P J 2013 *Biotechnol. J.* **8** 327−37

[54] Carrasco E, Jiménez-Redondo M, Tanarro I and Herrero V J 2011 *Phys. Chem. Chem. Phys.* **13** 19561−72

[55] van Helden J H, van den Oever P J, Kessels W M M, van de Sanden M C M, Schram D C and Engeln R 2007 *J. Phys. Chem.* A **111** 11460−72

[56] Peter S, Pintaske R, Hecht G and Richter F 1993 *J. Nucl. Mater.* **200** 412−6

[57] Lieberman A L and Lichtenberg A J 1994 *Principles of Plasma Discharges and Material Processing* (New York: Wiley)

[58] Schröder K, Meyer-Plath A, Keller D, Besch W, Babucke G and Ohl A 2001 *Contrib. Plasma Phys.* **41** 562−72

[59] Meyer-Plath A A, Schröder K, Finke B and Ohl A 2003 *Vacuum* **71** 391−406

Meyer-Plath A A, Schröder K, Finke B and Ohl A 2003 *Symp. on Plasma Surface Engineering at the Spring Meeting of the German Physical Society* (Regensburg, Germany, March 11−15 2002)

[60] Miyayama T, Sanada N, Bryan S R, Hammond J S and Suzuki M 2010 *Surf. Interface Anal.* **42** 1453−7

[61] Paynter R W 2009 *Surf. Interface Anal.* **41** 595−601

[62] Lock E H, Petrovykh D Y, Mack P, Carney T, White R G, Walton S G and Fernsler R F 2010 *Langmuir* **26** 8857−68